Gas heating in low-pressure microwave argon discharges

A. Palmero,[1] J. Cotrino,[1] C. Lao,[2] and A. R. González-Elipe[1]
[1]*Departamento de Física Atómica, Molecular y Nuclear, Facultad de Física, Universidad de Sevilla, Sevilla, Spain and Instituto de Ciencias de Materiales, Isla de la Cartuja, Sevilla, Spain*
[2]*Departamento de Física Aplicada, Universidad de Córdoba, Córdoba, Spain*
(Received 15 April 2002; published 3 December 2002)

Both an energy balance equation and a collisional-radiative model were developed in order to discover which process is responsible for gas heating in a low-pressure argon discharge. In this way, for a wide range of plasma conditions, the space-charge field contribution to gas heating was found to be negligible compared to that resulting from elastic collisional processes, although the value of the former is higher than the latter when calculating the absorbed power per electron. This is due to (1) the heating associated with the space-charge field only being effective in the plasma sheath, which is very close to the vessel inner wall. (2) The vessel temperature value at the external wall is taken as a boundary condition, as a result of which the space-charge field influence on gas heating is indirectly imposed on the model. The results of the collisional-radiative model take into account the influence of gas heating on the electron temperature and on the argon low-lying excited levels. Two different zones have been found. The first corresponds to low electron densities, in which the gas temperature remains constant, whereas in the second (high electron densities) the heating of the gas takes on great importance. These results compare well with experimental data.

DOI: 10.1103/PhysRevE.66.066401 PACS number(s): 52.20.−j, 52.20.Hv, 52.25.Dg, 52.40.Kh

I. INTRODUCTION

In recent years, gas heating due to the interaction between electrons and heavy particles has been proved to be very important in the characterization of low-pressure argon plasmas [1,2]. Indeed, gas temperature is a relevant parameter when studying neutral and ion properties, as well as the interaction of these species with another gas or with a solid surface. It is, therefore, necessary to characterize the mechanisms through which the heavy particles are heated, and this is the scope of this paper. Nevertheless, gas temperature has been shown to be different from environment temperature for values of electron densities above 10^{18} m^{-3}, and, therefore, interest is centered on microwave discharges, since the typical values of electron density are of the same order of magnitude in this case.

High-frequency low-pressure plasmas produced and sustained by a traveling wave have been proved to be suitable for many industrial applications, such as microelectronics, surface treatment, polymer modification, etching, sterilization and abatement processes, etc., [3–7]. These discharges, specifically those designed for microwave field applicators, are usually produced by a traveling electromagnetic wave that propagates along the interface between the plasma and a dielectric vessel (surface-wave plasmas). They display a considerable flexibility for experimental operations and are highly suitable for theoretical modeling.

Discharges sustained by surface waves in cylindrical geometry exhibit both radial and axial electron density gradients. The former are a product of the competition between ionization and diffusion processes leading to Bessel-like profiles, while the latter is governed by the coupling of the wave and the plasma, and produces nearly linear profiles [8,9]. However, the radial problem is usually avoided by using an average cross-section electron density with an important axial gradient. Moreover, the theoretical study of these discharges is generally divided into two parts: surface-wave propagation and plasma kinetics [10]. The first describes the propagation of the electromagnetic wave along the plasma column, while the second studies the collisional-radiative processes among the particles.

To data, several models have been published that deal with the population density of excited states and electrons. They state that plasma magnitudes, such as electron density and temperature (as well as the population density of excited states), are coupled to the energy transport of heavy particles, and that gas heating plays an important role in low-pressure plasma modeling. In Ref. [1] an energy transport equation was deduced for a low-pressure microwave argon plasma which showed the importance of the elastic processes between electrons and heavy particles in gas heating,

$$\frac{1}{r}\frac{\partial}{\partial r}\left(\lambda_T(T_g)\frac{\partial T_g}{\partial r}\right)=\theta_{el}n_e, \tag{1}$$

where T_g is the gas temperature, $\lambda_T(T_g)$ the gas thermal conductivity, n_e the electron density, and θ_{el} the power lost per electron in elastic collisions. The paper included all the important processes for evaluation except ion heating due to acceleration caused by the space-charge field. This effect can be important owing to the fact that the power required to maintain the space-charge field is usually higher than the power expended in elastic collisions between electrons and neutrals [11]. Therefore, a study of the influence of both processes would seem to be required in order to identify which is most responsible for gas heating.

The aim of this paper is to clarify which of these two processes (elastic collisions between electrons and heavy particles and ion heating due to the acceleration caused by the space-charge field) is responsible for gas heating in an argon low-pressure plasma column in typical conditions. To this end, we have obtained an energy balance equation that

 ©2002 The American Physical Society

calculates the gas temperature as a function of the plasma parameters and the vessel temperature at the external wall. Hence, it has been shown that the space-charge field contribution to gas heating is negligible compared to the contribution of the elastic processes, despite the fact that in the calculation of the total power lost by an electron, θ_L, the former is higher. This result stems from two causes, (1) the space-charge field is only appreciable in the plasma sheath, whereas the elastic processes contribute to the heating of the plasma bulk, and (2) the boundary condition (i.e., the vessel temperature at the external wall) is located very close to the surface where space-charge field heating is important, and therefore, its contribution is implicit in this value.

This paper is organized as follows: in Sec. II we deduce an energy balance equation and an 11-level collisional-radiative model has been developed for a low-pressure argon plasma. The discussion and the results—as well as a comparison with experimental data—are presented in Sec. III. Furthermore, in the same section, an approximate result of the gas energy balance equation is presented. Finally, the significance of these results is discussed in Sec. IV.

II. MODELING

In the following sections, a model of an argon plasma column is to be developed that includes an energy balance equation to take into account the gas heating due to the interaction between the electron population and the heavy particles. The conditions postulated for the development of this model are valid for many laboratory plasmas, and are as follows:

(1) The electromagnetic wave frequency is equal to 0 (dc discharge), or it is high enough to permit a stationary description of the plasma (high-frequency discharge). This implies that during the time the plasma takes to reach the steady-state situation, the electromagnetic field must oscillate many times. As a result of this, during the time the plasma evolves, the electrons only ''perceive'' an average value of the field.

(2) The mean free path of any particle in the plasma is much lower than any vessel size. Thus, either the thermal conduction or the diffusion of the particles can be described through temperature or particle density gradients, respectively.

(3) The charged particles diffusive regime is ambipolar, i.e., the electron flow towards the vessel wall must be equal to the positive ion flow. Therefore, the plasma can be considered quasineutral.

(4) Gas pressure is low enough to allow a description of the plasma through all the processes we have taken into account (see Table I). Indeed, if we consider a higher pressure range, other processes (as well as other species) must be included.

(5) The thickness of the plasma sheath must be much lower than any plasma dimension, so we can study its properties in the limit where it tends to zero. Furthermore, gas pressure is low enough to allow a noncollisional description of the plasma sheath.

On the basis of these assumptions we have developed an energy balance equation that will be obtained in the following section.

TABLE I. Collisional and radiative processes included in the model.

Reaction	Coefficient
$\mathrm{Ar}(i)+e\rightarrow \mathrm{Ar}(j)+e$	c_{ij}
$\mathrm{Ar}(i)+e\rightarrow \mathrm{Ar}^{+}+e+e$	$c_{i\lambda}$
$\mathrm{Ar}(i)\leftrightarrow A(j)+h\nu\ (j<i)$	A_{ij}^{ef}
e, Ar^{+} and Ar(1) diffusion	D

A. Energy balance equation

In this section, an energy balance equation for an argon plasma is deduced under the conditions listed in Sec. II. In this case, the kinetics is dominated by electron collisions with heavy particles and the ambipolar diffusion regime for electrons and ions, whereby

$$-D\vec{\nabla}n_e=n_e\vec{v}_e^{\,d}=n_{ion}\vec{v}_{ion}^{\,d}=-n_1\vec{v}_1^{\,d}, \tag{2}$$

where n_{ion} and n_1 are the argon ion density and the density of the argon atoms in the ground state, respectively, $\vec{v}_e^{\,d}$, $\vec{v}_{ion}^{\,d}$, and $\vec{v}_1^{\,d}$ the diffusion velocities of electrons, ions, and atoms, and D the ambipolar diffusion coefficient. Equation (2) represents the condition required to maintain neutrality in the plasma, whereby for each electron and ion that flows towards the wall, an argon atom in the ground state flows towards the center of the discharge. It will furthermore be assumed that transport is negligible for all the excited species.

It is assumed that the argon atom has N energy levels (ε_i denotes the energy level) and one free energy level (ε_λ), while the plasma kinetics can be properly described by the processes included in Table I [12]. Therefore, the kinetic coefficient corresponding to each process can be calculated when the electron energy distribution function (EEDF) and the cross section of the process are known. The radiative transport can be substantially simplified by using the Holstein escape factor concept, Λ, defined as $A_{ij}^{ef}=\Lambda A_{ij}$, where A_{ij} is the Einstein coefficient for the transition [13,14]. In this way, the kinetic equation that describes the time variation of the population density of the i level is written as

$$\frac{\partial n_i}{\partial t}=\sum_{j=1}^{N}c_{ji}n_jn_e-\sum_{j=1}^{N}c_{ij}n_in_e-c_{i\lambda}n_in_e-\sum_{j<i}A_{ij}^{ef}n_i+\sum_{j>i}A_{ji}^{ef}n_j\ \ (i=2,3,\ldots,N), \tag{3}$$

and for the electron density

$$\frac{\partial n_e}{\partial t}=\sum_{i=1}^{N}c_{i\lambda}n_in_e+\vec{\nabla}\cdot(D\vec{\nabla}n_e), \tag{4}$$

where

$$n_{ion} = n_e \tag{5}$$

and

$$\sum_{i=1}^{N} n_i + n_e = n_0; \tag{6}$$

here n_i is the population density of the i level, D the diffusion coefficient, and n_0 the population density of the particles of the plasma. In steady-state conditions we introduce the energy conservation equation for the electrons

$$\vec{\nabla} \cdot \left[n_e \vec{v}_e^{\,d} \left(\frac{3}{2} k_B T_e \right) \right] = \sigma E_{eff}^2 - \theta_L n_e ,$$

where σ is the electrical conductivity and E_{eff} the effective local field value. Using Eq. (2) we obtain

$$\sigma E_{eff}^2 = \theta_L n_e - \vec{\nabla} \cdot \left[D \vec{\nabla} n_e \left(\frac{3}{2} k_B T_e \right) \right], \tag{7}$$

with

$$\theta_L = \theta_{el} + \theta_{in} + \theta_w ,$$

where θ_{el} and θ_{in} are the elastic and inelastic contributions to θ_L, defined by

$$\theta_{el} = \frac{3m}{M} \nu_c k_B (T_e - T_g) \simeq \frac{3m}{M} \nu_c k_B T_e , \tag{8}$$

$$\theta_{in} = \sum_{i=1}^{N} \left[\sum_{\substack{j=1 \\ j \neq i}}^{N} c_{ij} n_i (\varepsilon_j - \varepsilon_i) + c_{i\lambda} n_i (\varepsilon_\lambda - \varepsilon_i) \right], \tag{9}$$

and θ_w is the power used to maintain the space-charge field. Here, ν_c is the effective collision frequency for momentum transfer between electrons and neutrals, T_e the electron temperature, and m and M the electron and argon atom masses, respectively. In Eq. (8) we have assumed $T_e \gg T_g$, which is valid for low-pressure discharges.

Hence, the power absorbed by the plasma per unit of volume is σE_{eff}^2. In the following several ways by which the plasma can lose power will be considered.

(1) *Radiative emission* (L_r). This is one of the ways the plasma can lose power per unit of volume. We can estimate this value through the model, obtaining the expression $L_r = \sum_{i=2}^{N} \sum_{j<i} A_{ij}^{ef} n_i (\varepsilon_i - \varepsilon_j)$,

(2) *Heat conduction* (L_h). Since the environment remains at a lower temperature than the plasma, heat conduction is another way by which the plasma loses power per unit of volume. Only the thermal flows associated with the gas temperature gradient, L_h, will be considered, since losses due to electron heat conduction (electron temperature gradients) are negligible at low pressures. Therefore, we have $L_h = -\vec{\nabla} \cdot (\lambda_T \vec{\nabla} T_g)$, where λ_T is the argon thermal conductivity ($\lambda_T = 4.17 \times 10^{-4} T_g^{2/3}$ W K$^{-5./3}$ m^{-1}) [15].

(3) *Diffusive losses* (L_d). The power flow due to the ambipolar diffusive regime, $\vec{\Gamma}_d$, can be expressed as

$$\vec{\Gamma}_d = n_e \vec{v}_e^{\,d} \left(\varepsilon_\lambda + \frac{3}{2} k_B T_e + \frac{3}{2} k_B T_g \right) + n_1 \vec{v}_1^{\,d} \left(\varepsilon_1 + \frac{3}{2} k_B T_g \right),$$

and using Eq. (2) we find

$$\vec{\Gamma}_d = -D \vec{\nabla} n_e \left(\varepsilon_\lambda - \varepsilon_1 + \frac{3}{2} k_B T_e \right).$$

Therefore, the power lost per unit of volume, L_d, is

$$L_d = \vec{\nabla} \cdot \vec{\Gamma}_d = -\vec{\nabla} \cdot \left[D \vec{\nabla} n_e \left(\varepsilon_\lambda - \varepsilon_1 + \frac{3}{2} k_B T_e \right) \right].$$

In a steady-state situation, absorbed microwave power must be equal to dissipated power, and therefore $\sigma E_{ef}^2 - (L_h + L_r + L_d) = 0$ must hold. Thus, the following equation can be obtained:

$$\sigma E_{ef}^2 + \vec{\nabla} \cdot (\lambda_T \vec{\nabla} T_g) - \sum_{i=2}^{N} \sum_{j<i} A_{ij}^{ef} n_i (\varepsilon_i - \varepsilon_j) + \vec{\nabla} \cdot \left[D \vec{\nabla} n_e \left(\varepsilon_\lambda - \varepsilon_1 + \frac{3}{2} k_B T_e \right) \right] = 0. \tag{10}$$

Using Eqs. (3)–(6) and Eq. (9), we have

$$\theta_{in} n_e = \sum_{i=2}^{N} \sum_{j<i} A_{ij}^{ef} n_i (\varepsilon_i - \varepsilon_j) - \vec{\nabla} \cdot (D \vec{\nabla} n_e)(\varepsilon_\lambda - \varepsilon_1),$$

and from Eq. (7) and Eq. (10) we obtain the energy balance equation, which is

$$\vec{\nabla} \cdot (\lambda_T \vec{\nabla} T_g) + (\theta_{el} + \theta_w) n_e = 0. \tag{11}$$

To solve Eq. (11), we need a full description of the plasma discharge since the values of θ_{el} and θ_w must be known. This problem can be simplified by taking into account that the space-charge field is only important within the plasma sheath (which is very close to the inner vessel wall) the size of which is, approximately, a few Debye lengths, $\lambda_D = (\varepsilon_0 k_B T_e / n_e e^2)^{1/2}$. Indeed, if we assume the Debye length to be much lower than any plasma dimension, we can write

$$\theta_w \simeq v_B e V \delta(\vec{r} - \vec{r}_{wall}),$$

where V is the wall potential, e the electron charge, v_B the Bohn velocity, $\vec{r}_{wall}$ a vector marking the inner vessel surface, and δ the Dirac function. Conversely, in the vessel volume the following equation holds:

$$\vec{\nabla} \cdot (\lambda_v \vec{\nabla} T_v) = 0,$$

where T_v is the vessel temperature and λ_v the vessel thermal conductivity. Thus, we can write the energy balance equation for the plasma and the vessel as

$$\vec{\nabla} \cdot (\lambda \vec{\nabla} T) + (\theta_w + \theta_{el}) n_e = 0, \tag{12}$$

where we have $\lambda = \lambda_T$ in the plasma, and $\lambda = \lambda_v$, $n_e = \theta_{el} = 0$ in the vessel.

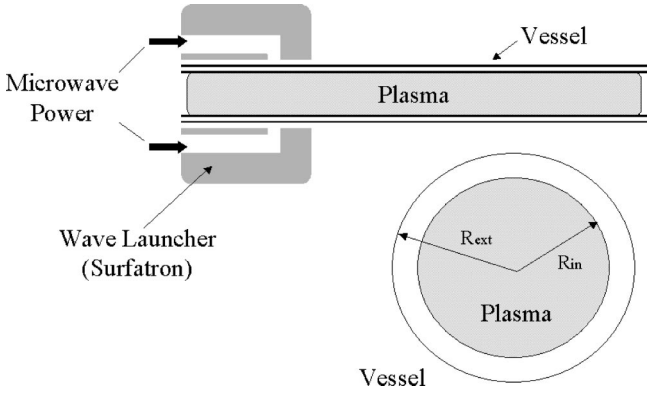

FIG. 1. Diagram of the argon plasma column studied in this paper.

B. Solution of the energy balance equation for a low-pressure argon plasma column

In order to solve Eq. (12) we have developed a collisional-radiative model of a low-pressure argon plasma cylindrical column (Fig. 1). In this case, the plasma axial length is much longer than its diameter, and the axial gradients can be disregarded compared to the radial gradients, so the energy balance equation remains

$$\frac{1}{r}\frac{\partial}{\partial r}\left(\lambda r\frac{\partial T}{\partial r}\right)+(\theta_{el}+\theta_w)n_e=0, \tag{13}$$

where r is the cylindrical coordinate, θ_{el} is given by Eq. (8) and $\theta_w=v_B eV\delta(r-R_{in})$, where $V=(k_BT_e/e)\ln(M/m)$ and $v_B=(k_BT_e/M)^{1/2}$ [16]. The boundary conditions are

$$\frac{\partial T}{\partial r}(r=0)=0$$

and

$$T(r=R_{ext})=T_{ext},$$

where T_{ext} is the vessel temperature at the external wall.

Naturally, Eq. (13) gives the same solutions as Eq. (1) for $0<r<R_{in}$. The only difference between them is the boundary condition, since in the latter case the internal vessel temperature, T_w, must be known, while for Eq. (13) the boundary condition is related to the vessel temperature at the external wall.

To simplify the results of these models, we will assume a J_0 Bessel radial profile for the electrons. This profile has been shown suitable to describe the electron population in many low-pressure situations [8,9,17,18]. We therefore have

$$n_e(r,z)=\frac{R_{in}^2}{2}\frac{J_0\left(\frac{r}{R_{in}}\alpha\right)}{\int_0^R drrJ_0\left(\frac{r}{R_{in}}\alpha\right)}\langle n_e\rangle(z),$$

where $\langle n_e\rangle(z)$ is the radial average electron density at the axial position z, and α is a parameter whose value is obtained through the Bohn condition at the wall

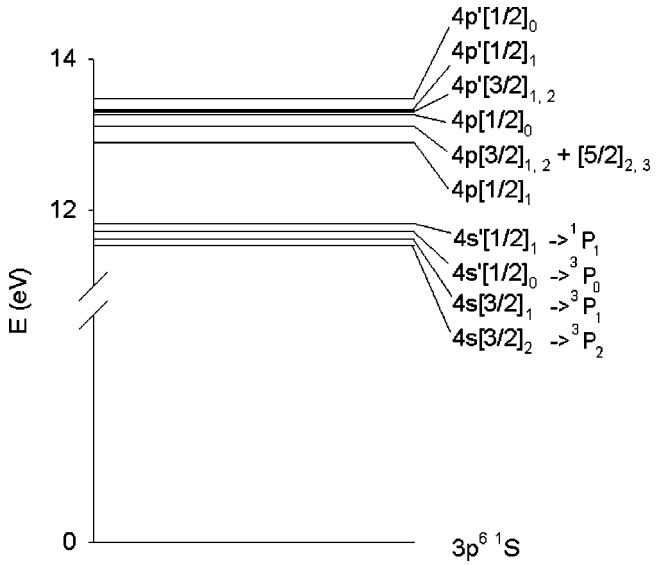

FIG. 2. Scheme of the argon excited levels included in the model.

$$v_{ion}^d(r=R_{in})=v_B.$$

The argon atom has been described through an 11-level model (Fig. 2), including the ground state, all the $4s$ and $4p$ levels, and the ionized level. High-lying levels have not been taken into account since, in most cases, they remain in a partial local Saha equilibrium; we are therefore interested in low-lying levels [19,20].

Moreover, the kinetic coefficients, c_{ij}, can be calculated using the expression

$$c_{ij}=\sqrt{\frac{2}{m_e}}\int_{\Delta\varepsilon_{ij}}^{\infty}duf(u)\sigma_{ij}(u)u,$$

where $\Delta\varepsilon_{ij}$ is the threshold energy, $f(u)$ the EEDF, normalized as $\int_0^\infty du\sqrt{u}f(u)=1$, and $\sigma_{ij}(u)$ the cross section for the process

$$\sigma_{ij}(u)=\sigma_{ij}^A(u)+\sigma_{ij}^S(u)+\sigma_{ij}^P(u),$$

where $\sigma_{ij}^A(u)$ is the cross section for optically allowed transitions and $\sigma_{ij}^S(u)$, $\sigma_{ij}^P(u)$ the cross sections for spin and parity forbidden transitions, respectively [21]. To obtain the kinetic coefficients, c_{ij}, we have assumed that the EEDF is Maxwellian. This approximation is only valid when the electron-electron elastic interaction becomes important when solving the Boltzmann equation, and, therefore, when we have a high electron density in the discharge [22].

Hence, by knowing the radial average electron density value at the axial position z, $\langle n_e\rangle(z)$, the external vessel temperature, T_{ext}, and the gas pressure, the model can be solved and the population of the low-lying excited states can be obtained as well as the gas and electron temperatures and their radial profile.

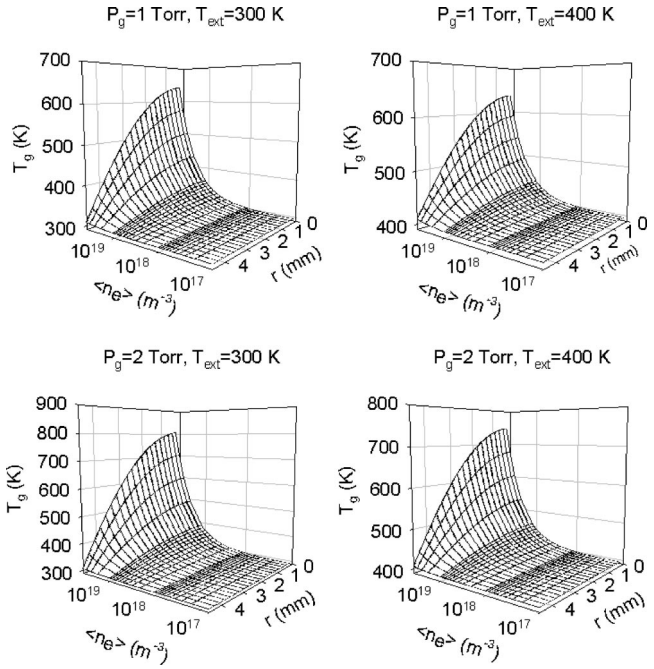

FIG. 3. Radial profile of the gas temperature as a function of the radial average electron density for gas pressures of 1 and 2 Torr, and for vessel temperatures at the external wall of 300 and 400 K. In all cases $R_{in}=4.5$ mm and $R_{ext}=6$ mm.

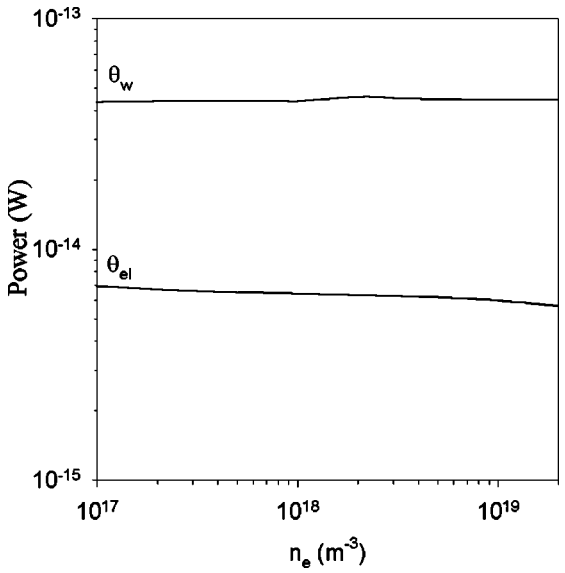

FIG. 4. Typical values of θ_{el} and $\langle \theta_w \rangle$ as a function of the radial average electron density.

III. RESULTS AND DISCUSSION

A. Theoretical results

The gas temperature values have been calculated at a gas pressure of 1 and 2 Torr as a function of $\langle n_e \rangle(z)$ in two cases, $T_{ext}=300$ K and $T_{ext}=400$ K, by postulating a vessel made of Pyrex with inner and outer radii of 4.5 and 6 mm, respectively (Fig. 3). In all the cases that we have studied, the differences between the vessel temperature at the inner and external wall were always less than 10 K, and therefore the relative error when assuming $T_w \simeq T_{ext}$ was below 3% ($T_{ext}-T_w/T_{ext} \leqslant 0.03$). As a conclusion, the results obtained when solving Eq. (12) for $0<r<R_{ext}$ with $T(R_{ext})=T_{ext}$ are practically identical to those obtained for $0<r<R_{in}$ when assuming $T(R_{in})=T_w \simeq T_{ext}$. Thus, the gas temperature values that we have obtained through the model are similar to those presented in Ref. [1], although $\langle \theta_w \rangle$ is much higher than θ_{el} (Fig. 4).

The radial average electron temperature as a function of the electron density is shown in Fig. 5 for the same working conditions than those of Fig. 3. In this case we find two important zones: zone 1 (low and intermediate electron densities, $n_e \leqslant 10^{18}$ m^{-3}), in which the gas heating is not important, and the gas temperature is very close to the vessel temperature, and zone 2 (high electron densities $n_e \gtrsim 10^{18}$ m^{-3}), where the gas temperature notably increases. Naturally, the boundary between these two zones can only be taken as approximate.

Hence, the value of the electron density determines the gas temperature, and therefore, the density of particles in the plasma, n_0. Indeed, in the first zone, n_0 remains almost constant and independent of the electron density, whereas in the second, it decreases as the electron density increases. Thus, in the first zone the results are equivalent to those obtained using a constant gas temperature model in a typical ionization-diffusion regime. The electron temperature, therefore, decreases as the electron density increases (due to the fact that the more electrons in the discharge, the less energy is needed to maintain the ionization rate). In addition, in zone 2 this trend changes because n_0 decreases when the electron density increases, so the electron temperature rises.

Conversely, the population of the excited states will be determined by considering two mechanisms: the excitation processes due to collisions between neutrals and electrons, and the variation of the neutral population as a consequence

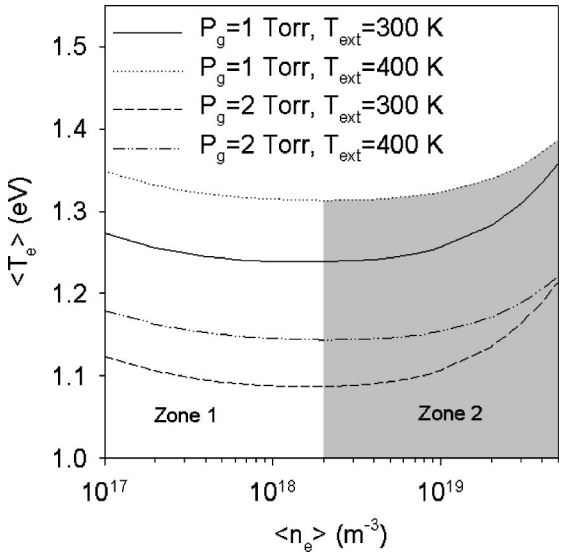

FIG. 5. Radial average electron temperature as a function of the radial average electron density for gas pressures of 1 and 2 Torr and for vessel temperatures at the external wall of 300 and 400 K. In all cases $R_{in}=4.5$ mm and $R_{ext}=6$ mm.

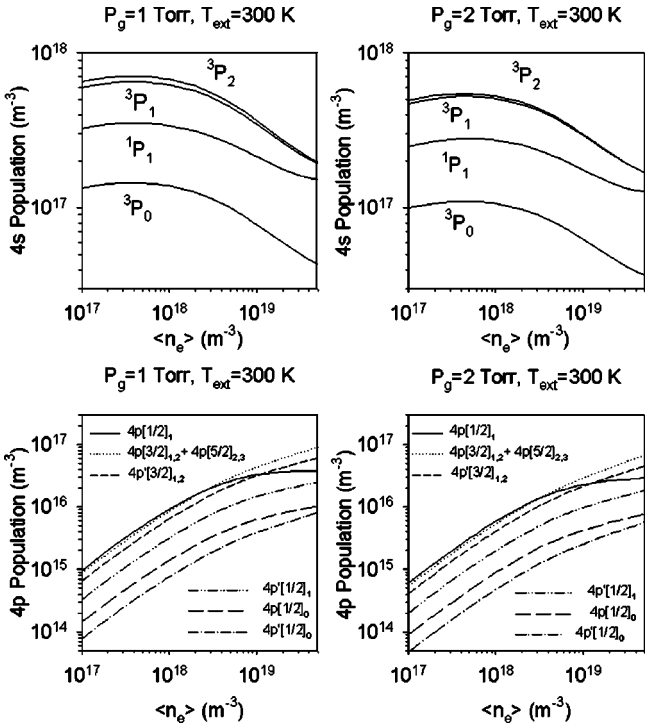

FIG. 6. Radial average values of the $4s$ and $4p$ excited states' population densities as a function of the radial average electron density for gas pressures of 1 and 2 Torr, and for a vessel temperature at the external wall of 300 K. In all cases $R_{in}=4.5$ mm and $R_{ext}=6$ mm.

of gas heating. In Fig. 6 we have represented the radial average values of the $4s$ and $4p$ excited states as a function of the radial average electron density. We find three different trends (Fig. 7): for low electron densities ($n_e \sim 10^{16}$ m^{-3}), the excitation mechanism is mainly governed by excitations from the ground state. Therefore, the excited states population increases as the electron density increases. For intermediate electron densities ($n_e \sim 10^{17}$–10^{18} m^{-3}), the main excitation and ionization mechanism is produced by electron impact with a neutral particle in the $4s$ state. Therefore, the $4s$ population decreases whereas the $4p$ population increases in accordance with the electron density. For high electron densities ($n_e \gtrsim 10^{19}$ m^{-3}), ionization is produced by electron collisions through the path $\mathrm{Ar}+e \rightarrow \mathrm{Ar}(4s)+e \rightarrow \mathrm{Ar}(4p)+e \rightarrow \mathrm{Ar}^{+}+e+e$, at the beginning of a "ladderlike" excitation mechanism. The $4s$ population decreases in accordance with the electron density, while the $4p$ population increases, due to the strong coupling between the $4s$ and $4p$ levels. Finally, for higher electron densities, the excited levels above the $4p$ levels may play an important role in the excitation and ionization mechanisms, and therefore a more detailed and extended model would have to be developed to include those levels.

B. Comparison between theoretical and experimental data

As has been proved in the preceding section, gas heating becomes important at high electron densities (above 10^{18} m^{-3}). Therefore, interest when comparing these results with experimental data is centered on conditions where the electron density may be of the same order of magnitude or higher. We have, therefore, compared the results of the model with experimental data for an argon plasma column produced by a surfatron for gas pressures above 1 Torr with inner and external radii of 4.5 and 6 mm, respectively. In this case, we have an argon surface-wave-produced and surface-wave-maintained plasma column with an electron density ranging between, approximately, 10^{17} and 10^{19} m^{-3} which is suitable for our purposes.

In Ref. [23] the electron temperature was obtained experimentally for pressures of 0.8, 1.1, 1.8, and 2.8 Torr, for an argon plasma produced in a tube with inner and external radii

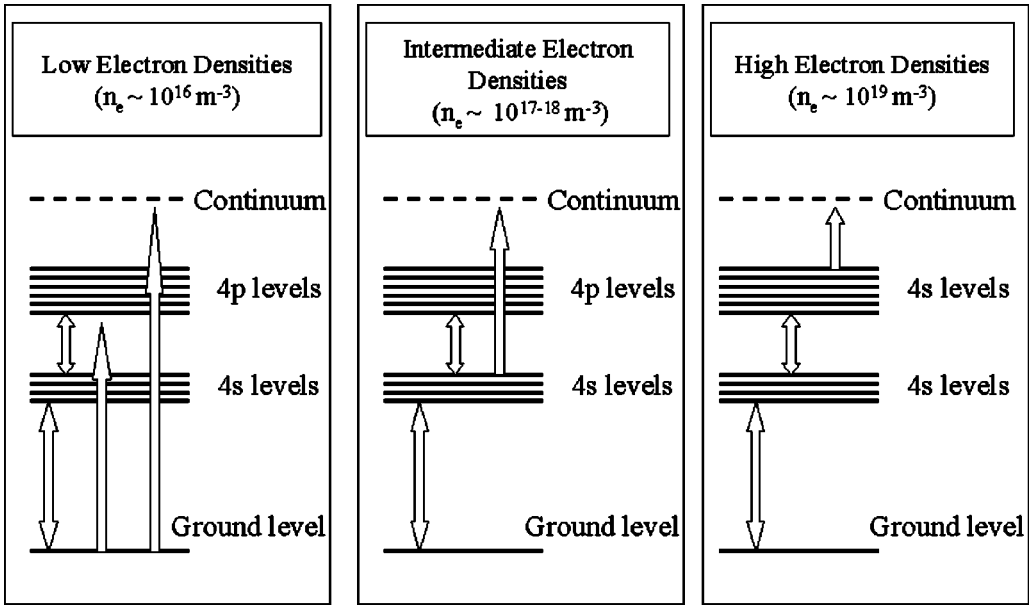

FIG. 7. Most important excitation and ionization processes depending on the electron density calculated through the model.

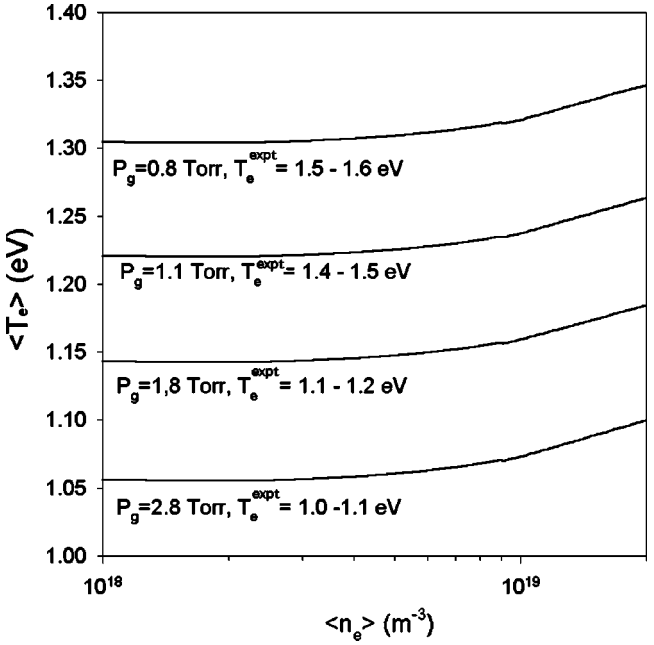

FIG. 8. Electron temperature calculated through the model as a function of the radial average electron density for different gas pressures. The vessel temperature at the external wall was 300 K, $R_{in}=4.5$ mm and $R_{ext}=6$ mm. Experimental values of the electron temperature in the same conditions are presented by the symbol T_e^{expt} [23]. The comparison between experimental and calculated values agrees in the cases of 1.8 and 2.8 Torr.

of 4.5 and 6 mm, respectively. Furthermore, the method used in the paper assumed that the EEDFs were Maxwellian, as a result of which, the Boltzmann equation had to be solved in the two terms approximation. In conclusion, the Maxwellian approximation was found to be valid throughout the whole pressure range, although the values obtained for 0.8 and 1.1 Torr were at the limit of said approximation. The results are shown in Fig. 8. In this figure, we find that the solution of the model reproduces the experimental data for gas pressures of 1.8 and 2.8 Torr, whereas for gas pressures of 0.8 and 1.1 Torr, the calculated electron temperatures are 20% below the experimental values. Such differences for the lower pressures are obtained because in both cases the Maxwellian approximation is not suitable for describing the plasma, owing to the fact that the electron density is still low in that pressure range.

We have also compared the results of the model with experimental data concerning the excited states populations [24]. In this case, the main problem when obtaining such results is the experimental evidence of self-absorption for the $4p$-$4s$ radiative transitions. This means that the escape factors for these transitions should be included with values of less than 1. However, the radiative transport in the plasma is not within the scope of this paper, and we will assume the thin plasma approximation for the transitions between the $4p$ and the $4s$ levels $[\Lambda(4p\rightarrow 4s)=1]$. Conversely, the escape factor for the transitions between the radiative $4s$ levels and the ground level are calculated by the formula

$$\Lambda=\Lambda_d e^{-\Lambda_{cd}/\Lambda_c^2}+\Lambda_c\ \mathrm{erf}\left(\frac{\Lambda_{cd}}{\Lambda_c}\right),$$

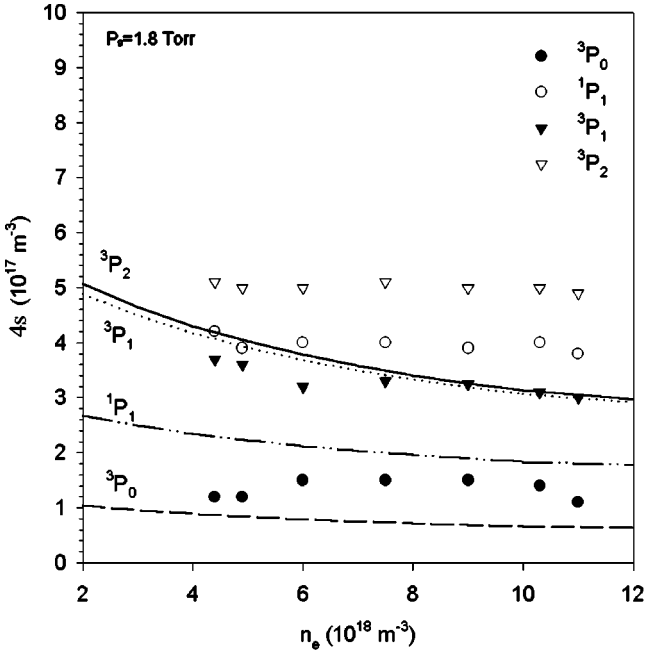

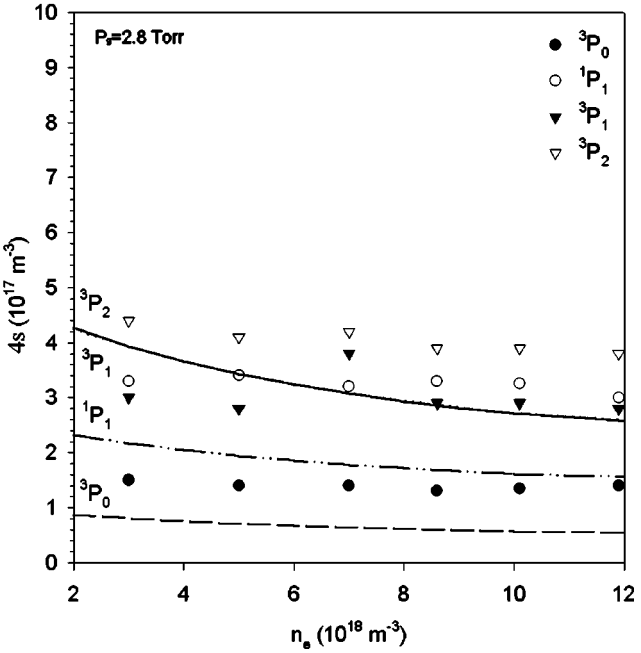

FIG. 9. Experimental values of the population of the argon $4s$ excited levels obtained in Ref. [24] along with the results of the model in the same conditions (gas pressures of 1.8 and 2.8 Torr, vessel temperature at the external wall of 300 K, $R_{in}=4.5$ mm and $R_{ext}=6$ mm).

where Λ_d and Λ_c are the pure Doppler and collisional escape factors, respectively, and Λ_{cd} is the escape factor for the combined action of both effects [13,14].

In Fig. 9 we have compared the experimental values of the $4s$ states with the theoretical data for gas pressures of 1.8 and 2.8 Torr in the same conditions as Fig. 3, i.e., we assume that the EEDF is Maxwellian. For these two pressures the results are good, highlighting the fact that the error incurred when disregarding self-absorption is lower that the experi-

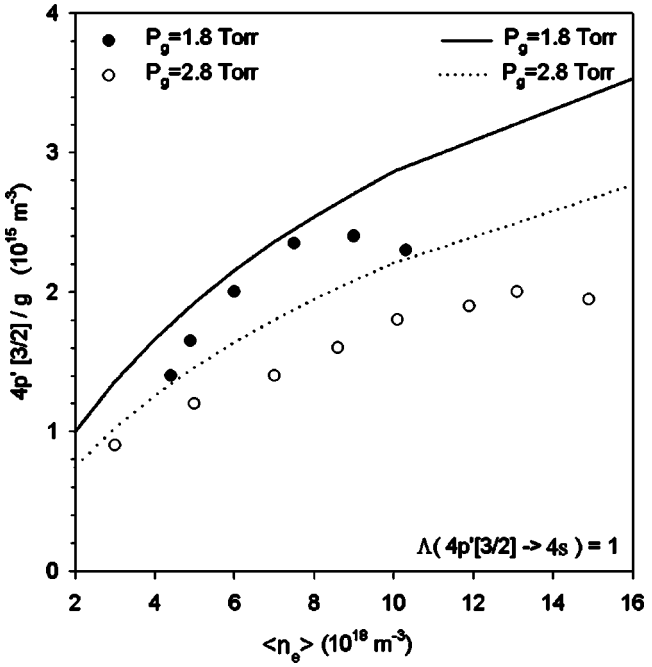

FIG. 10. Experimental values of the population of the $4p'[3/2]$ level, corresponding to the $4p$ levels, per unit of statistical weight [24] along with the results of the model in the same conditions (gas pressures of 1.8 and 2.8 Torr, vessel temperature at the external wall 300 K, $R_{in}=4.5$ mm and $R_{ext}=6$ mm).

mental error (20%). Moreover, the fact that they are always ordered in the same way suggests that the interchange between the theoretical and experimental values of the $^1P_1$ and $^3P_1$ levels might be caused by self-absorption. Indeed, the model can produce similar results if we assume that the escape factor of some transitions is lower than the unit. In Fig. 10 we show the theoretical and experimental results of the $4p'[3/2]$ population per unit of statistical weight in the same conditions as Fig. 3. In both cases good results were obtained.

C. Approximate solutions of the energy balance equation

In general, solving Eq. (1) implies developing a collisional-radiative model similar to that which we have presented in this paper. Nevertheless, it is interesting to analyze two simple cases that will help more complex situations to be understood. Indeed, although Eq. (13) allows the value of the gas temperature in a low-pressure discharge to be found, the problem is not easy to deal with, due to the coupling between the plasma magnitudes. In addition, in many axial models the radial problem is usually avoided by using radial average values, and therefore, an analytic expression between the radial average gas temperature and the plasma parameters is useful, despite the fact that some broad approximations are required. To overcome this problem, we will assume the following approximations:

$$T_e(r)\simeq\langle T_e\rangle,$$

$$\theta_{el}(T_e,T_g)\simeq\theta_{el}(\langle T_e\rangle,T_{ext}),$$

and

$$\lambda_T(T_g)\simeq\lambda_T,$$

where $\langle T_e\rangle$ is the radial average electron temperature. We will study two cases: (i) when the electron density radial profile is constant, and (ii) when the electron density radial profile has a J_0 Bessel shape.

1. Homogeneous electron density profile

In this case we assume

$$n_e\simeq\langle n_e\rangle,$$

and therefore, the solution of Eq. (13) is

$$T(r)=T_w-\frac{\theta_{el}\langle n_e\rangle}{4\lambda_T}(r^2-R_{in}^2),\quad 0<r<R_{in},$$

and

$$T(r)=T_{ext}+\frac{T_w-T_{ext}}{\ln\dfrac{R_{in}}{R_{ext}}}\ln\frac{r}{R_{ext}},\quad R_{in}<r<R_{ext},$$

where T_w is the temperature value at R_{in}. In addition, using the properties of the δ function, we can obtain

$$T_w=T_{ext}+\frac{R_{in}^2\langle n_e\rangle(\langle\theta_w\rangle+\theta_{el})}{2\lambda_v}\ln\left(\frac{R_{ext}}{R_{in}}\right),$$

where $\langle\theta_w\rangle=2v_BV/R_{in}$ is the radial average value of θ_w. Thus, the radial average gas temperature as a function of the temperature of the vessel at the inner wall, T_w, is

$$\langle T_g\rangle=T_w+\frac{\theta_{el}\langle n_e\rangle R_{in}^2}{8\lambda_T},$$

and as a function of the vessel temperature at the external wall

$$\langle T_g\rangle=T_{ext}+\frac{\langle n_e\rangle\theta_{el}R_{in}^2}{8\lambda_T}(1+\chi)+\frac{\langle n_e\rangle\langle\theta_w\rangle R_{in}^2}{8\lambda_T}\chi;\quad(14)$$

here we have introduced the function χ defined by

$$\chi=\frac{4\lambda_T}{\lambda_v}\ln\left(\frac{R_{ext}}{R_{in}}\right).$$

Equation (14) allows an estimate of the contribution of the elastic collisional processes to the gas heating, η_{el}, for a given external temperature

$$\eta_{el}=\frac{\frac{\langle n_e\rangle\theta_{el}R_{in}^2}{8\lambda_T}(1+\chi)}{\frac{\langle n_e\rangle\theta_{el}R_{in}^2}{8\lambda_T}(1+\chi)+\frac{\langle n_e\rangle\langle\theta_w\rangle R_{in}^2}{8\lambda_T}\chi}=\frac{1}{1+\frac{\langle\theta_w\rangle}{\theta_{el}}\frac{\chi}{(1+\chi)}}.$$

Thus, if we assume a vessel with $R_{in}=4.5$ mm and $R_{ext}=6$ mm, the quotient $\langle\theta_w\rangle/\theta_{el}$ is always less than 10 (Fig. 3), while the value of χ is about 0.02. We therefore find that the elastic processes are responsible for more than 90% of gas heating for a given value of the external vessel temperature, although the contribution of θ_w to θ is higher than θ_{el}. In this case, the fact that θ_w is only important in the plasma sheath, whereas θ_{el} is the dominant term in the plasma bulk, makes the latter more effective. Indeed, the space-charge field is responsible for the vessel heating, and accounts for the value of T_{ext}, while the elastic collisions are responsible for heating the gas volume. In all the cases we have solved, and for a given value of T_{ext}, the elastic contribution was responsible for more than 90% of gas heating.

2. Electron density J_0 Bessel profile

In this case, we assume

$$n_e=\frac{R_{in}^2}{2}\frac{J_0\left(\frac{r}{R_{in}}\alpha\right)}{\int_0^{R_{in}}drrJ_0\left(\frac{r}{R_{in}}\alpha\right)}\langle n_e\rangle,$$

with $\alpha\simeq\alpha_0$, where $\alpha_0=2.405$ is the first root of the J_0 Bessel function. The electron density at the vessel inner wall is therefore zero, and hence, we are neglecting the influence of the space-charge field on gas heating. We find that the radial average gas temperature can be expressed,

$$\langle T_g\rangle=T_w+\frac{\theta_{el}\langle n_e\rangle R_{in}^2}{\lambda_T\alpha_0^2},\tag{15}$$

as a function of the vessel temperature at the inner wall, whereas as a function of the vessel temperature at the external wall, it is

$$\langle T_g\rangle=T_{ext}+\frac{\theta_{el}\langle n_e\rangle R_{in}^2}{\lambda_T\alpha_0^2}\left(1+\frac{\alpha_0^2}{8}\chi\right),$$

since $\alpha_0^2\chi/8\ll 1$ in all the cases we have solved, the result is

$$\langle T_g\rangle=T_{ext}+\frac{\theta_{el}\langle n_e\rangle R_{in}^2}{\lambda_T\alpha_0^2}.\tag{16}$$

Equation (15) has also been obtained in Ref. [1], and has been proved to be suitable for reproducing the gas temperature values when the inner vessel temperature is known. Conversely, Eq. (15) is equal to Eq. (16) if we assume $T_w\simeq T_{ext}$.

Equation (16) is valid for each axial position along the plasma length. Furthermore, an important relationship between the average gas temperature and the plasma magnitudes can be found through this equation in the conditions of a surface-wave discharge. In fact, if we assume a constant axial electron temperature, we can multiply Eq. (16) by $1/l_p$ (where l_p is the plasma length) and by integrating axially from 0 to l_p we obtain

$$\overline{T_g}=T_{ext}+\frac{\theta_{el}}{\lambda_T\pi\alpha_0^2}\frac{N_e}{l_p},$$

where N_e is the total number of electrons in the discharge, and $\overline{T_g}$ the average (radial and axial) value of the gas temperature. A relationship can also be found between the incident microwave power at the gap and N_e if we assume a constant axial value of θ,

$$N_e=\frac{P_{inc}(0)}{\theta},$$

so we finally obtain

$$\overline{T_g}=T_{ext}+\frac{\theta_{el}}{\lambda_T\pi\theta\alpha_0^2}\frac{P_{inc}(0)}{l_p}.$$

Thus, if we produce a surface-wave plasma column and change the incident power (and consequently its length), the average gas temperature must obey the linear equation

$$\overline{T_g}=T_{ext}+b(P_g)\frac{P_{inc}(0)}{l_p},$$

where P_g is the gas pressure, with

$$b(P_g)=\frac{\theta_{el}}{\lambda_T\pi\theta\alpha_0^2}.$$

In addition, this linear behavior between the average gas temperature and the ratio $P_{inc}(0)/l_p$ has been observed experimentally in Refs. [2,25].

IV. CONCLUSIONS

In this paper, a gas energy balance equation for a low-pressure argon plasma has been deduced under some general conditions. This equation takes into account elastic and inelastic collisional processes, as well as the space-charge field contribution. We have solved this equation in the typical conditions of a low-pressure argon plasma column, and we have found that although the power required to maintain the space-charge field is much higher than that of the elastic processes, the latter are mainly responsible for heating the gas. This result is based on two facts: (i) the space-charge field is only appreciable in the interface between the plasma and the vessel (plasma sheath), and (ii) the vessel tempera-

ture at the external wall has been taken as a boundary condition, whereby the space-charge field influence on gas heating is indirectly imposed on the model. In addition, we have found that, in general, we can approximate the inner vessel temperature to the external vessel temperature. These results were obtained by solving the gas temperature equation under some broad approximations, as well as by coupling a kinetic model to this equation.

We have developed an 11-level collisional-radiative model and we have solved the energy balance equation for a low-pressure argon plasma column. Two zones have been found: the first (low and intermediate electron densities, $n_e \leqslant 10^{18}$ m^{-3}) in which the gas temperature is always equal to the vessel temperature; the second (high electron densities, $n_e \gtrsim 10^{18}$ m^{-3}) where the gas temperature increases in accordance with the electron density. In zone 1 the electron temperature decreases when the electron density increases, whereas in zone 2 the behavior is exactly the opposite.

The results of the theoretical model highlight the fact that low-lying excited states maintain different kinetic equilibriums. In this way, the $4s$ levels tend to increase for very low electron densities, due to the importance of the excitation from the ground level, which is typical of a corona balance. As the electron density becomes higher, the $4s$ populations decrease due to a new regime, the so-called excitation-saturation-balance regime, that makes them responsible for excitations and ionizations. At very high electron densities, the $4p$ levels are now responsible for ionizations due to ''ladderlike'' processes. Nevertheless, the $4p$ levels always tend to increase in accordance with the electron density. In all the cases we have solved, gas heating does not change these trends, but it does become relevant in zone 2.

Finally, the results of the model have been compared to experimental data of a surface-wave plasma produced by a surfatron, obtaining good results. As such, the theoretical electron temperature has been shown to be very close to experimental values when the EEDF is Maxwellian. In addition, the excited level population also agrees with experimental data in the same conditions.

ACKNOWLEDGMENT

This research was partially supported by Grants Nos. MAT2001-2820 and PPQ2001-3108 from the Dirección General de Investigación Científica y Técnica (Spain).

[1] A. Palmero, J. Cotrino, A. Barranco, and A. R. González-Elipe, Phys. Plasmas **9**, 358-363 (2002).
[2] A. Rousseau, E. Teboul, M. J. van der Sande, and J. A. M. van der Mullen, Plasma Sources Sci. Technol. **11**, 47 (2002).
[3] L. Paquin, D. Masson, M. R. Wertheimer, and M. Moisan, Can. J. Phys. **63**, 831 (1985).
[4] C. F. M. Borges, S. Schelz, L. Martin, and M. Moisan, Diamond Relat. Mater. **4**, 149 (1995).
[5] G. Sauvé, M. Moisan, J. Paraszczak, and J. Heidenreich, Appl. Phys. Lett. **53**, 470 (1988).
[6] R. Claude, M. Moisan, and M. R. Wertheimer, Appl. Phys. Lett. **50**, 1797 (1987).
[7] S. Moreau, M. Moisan, M. Tabrizian, J. Barbeau, J. Pelletier, A. Ricard, and L. H. Yahia, J. Appl. Phys. **88**, 1166 (2000).
[8] Z. Zakrzewski, M. Moisan, V. M. M. Glaude, C. Beadry, and P. Leprince, Plasma Phys. **19**, 77 (1977).
[9] M. Böbe, G. Himmel, I. Koleva, and M. Schlüter, J. Phys. D **32**, 2426 (1999).
[10] E. Benova, Ts. Petrova, A. Blagoev, and I. Zhelyazkov, J. Appl. Phys. **84**, 147 (1998).
[11] J. Henriquez, E. Tatarova, F. M. Dias, and C. M. Ferreira, J. Appl. Phys. **90**, 4921 (2001).
[12] M. Mitchner and Charles H. Kruger, *Partially Ionized Gases* (Wiley, New York, 1973), p. 426.
[13] T. Holstein, Phys. Rev. **72**, 1212 (1947).
[14] T. Holstein, Phys. Rev. **83**, 1159 (1951).
[15] Yu. B. Goluboskii, Sov. Phys. Tech. Phys. **24**, 173 (1979).
[16] C. Lee and M. A. Lieberman, J. Vac. Sci. Technol. A **13**, 368 (1995).
[17] C. M. Ferreira, J. Phys. D **22**, 705 (1989).
[18] E. Benova, Ts. Petrova, A. Blagoev, and I. Zheliazkov, J. Appl. Phys. **59**, 1466 (1986).
[19] S. Nowak, J. A. M. van der Mullen, B. van der Sijde, and D. C. Schram, J. Quant. Spectrosc. Radiat. Transf. **41**, 177 (1989).
[20] H. A. G. Fey, W. W. Stoffels, J. A. M. van der Mullen, B. van der Sijde, and D. C. Schram, Spectrochim. Acta, Part B **46**, 885 (1991).
[21] A. Bogaerts, R. Gijbels, and J. Vlcek, J. Appl. Phys. **84**, 121 (1998).
[22] C. M. Ferreira and J. Loureiro, J. Phys. D **17**, 1175 (1984).
[23] C. Lao, J. Cotrino, A. Palmero, and A. R. González-Elipe, Eur. Phys. J. D **14**, 361 (2001).
[24] C. Lao, Ph.D. thesis, Seville University, 1998 (unpublished).
[25] A. Palmero, J. Cotrino, C. Lao, A. Barranco, and A. R. González-Elipe, Jpn. J. Appl. Phys. **41**, 5787 (2002).